Kamlet–Taft. pi. * polarizability/dipolarity of mixtures of water with various organic solvents

2 AUTHORS:

Won Jo Cheong
Inha University
93 PUBLICATIONS **1,122** CITATIONS

SEE PROFILE

Peter W Carr
University of Minnesota Twin Cities
424 PUBLICATIONS **13,517** CITATIONS

SEE PROFILE

Kamlet–Taft π* Polarizability/Dipolarity of Mixtures of Water with Various Organic Solvents

Won Jo Cheong and Peter W. Carr*

Department of Chemistry, Smith and Kolthoff Halls, University of Minnesota, 207 Pleasant Street, Minneapolis, Minnesota 55455

The Kamlet–Taft π* values of mixtures of water with four organic solvents over the entire range of composition have been estimated by solvatochromic measurements with a series of carefully selected indicators. The measured π* value of each indicator is collinear with the average π* value. We interpret these results as indicating that the indicators sense the polarizability/dipolarity and not the hydrogen bond acidity of the solvent. Examination of relationships between π* and ε and between E_T and π* and excess properties of π*, E_T, and ε with respect to volume fraction of the organic cosolvent leads to the conclusion that the principal effect of changing the solvent composition on the observed π* values operates through the dielectric properties of the local medium about the solute. This also supports the previous observation that solvatochromic shifts of the indicators used in this study are not very sensitive to solvent hydrogen bond acidity. The measured π* values together with literature E_T values were used to estimate α values, the hydrogen bond acidity parameter, of aqueous organic solvents.

The physical properties of water and aqueous mixtures of organic solvents are important for many reasons. In order to characterize solute–solvent dipolar interactions, we chose to use the Kamlet–Taft π* scale because this approach is experimentally one of the most well founded scales of solvent strength (1, 2). A solvent π* value is known to represent a blend of dipolarity and polarizability. Values are available for more than 200 solvents (2) including supercritical fluids, perfluorinated alkanes, several homologous series of liquids, and highly dipolar solvents such as dimethyl sulfoxide and acetonitrile. The relationship of π* to such fundamental electrostatic properties as dielectric strength (ε) and refractive index (n) has been explored in detail (3–8).

The π* parameter is obtained from measurements of the frequency of maximum absorption of at least three and often many more carefully selected indicators. In general the test solutes are disubstituted benzene derivatives. When π* is the solvent property of interest the indicators must be chosen to avoid or render negligible the effect of solute–solvent hydrogen bond (HB) complex formation on the indicator property. Two types of complexes can be identified: type A complexes are formed when the solute acts as an acceptor (base) and the solvent as a donor (acid); the converse situation defines a type B complex (2). In the case of solvatochromic measurements of solvent dipolarity, which based upon electronic spectroscopy, there must be no difference in the ability of the ground and excited states of the molecule to interact with the solvent. This is a very different condition than exists in using an equilibrium property such as a gas–liquid equilibrium constant to measure solvent dipolarity. For example to measure the π* of an HB base solvent the test solute may be an HB acid provided that the ground and excited state have no difference in their HB acidity. Obviously the weaker the interaction is in either state relative to the dipolar interaction, the less

Table I. Solvatochromic Characteristics of Pure Liquids

solvent	π^{*a}	α^b	β^c	ϵ^d	E_T^e	n^f
water	1.09 $(0.07)^g$	1.17 $(0.11)^h$	0.18^j	78.6	63.1	1.333
acetonitrile	0.75 $(0.03)^g$	0.19 $(0.08)^h$	0.31	36.2	45.6	1.342
methanol	0.60 $(0.03)^g$	0.93 $(0.08)^h$	0.62	32.2	55.5	1.327
2-propanol	0.50 $(0.04)^g$	0.76 $(0.07)^h$	0.95	17.7	48.2	1.378
THF	0.60 $(——)^i$	0.00	0.55	7.62	37.2	1.404

[a] Dipolarity/polarizability parameter from ref 2. [b] Hydrogen bond donating acidity from ref 2. [c] Hydrogen bond accepting basicity from ref 2. [d] Dielectric constants from ref 23 and 25. [e] Reichardt $E_T(30)$ from ref 16. [f] Refractive index from ref 23 and 25. [g] Standard deviation in π* from ref 9. [h] Standard deviation in α, unpublished work of R. W. Taft (35). [i] Not reported. [j] This value may be underestimated; private communication with R. W. Taft.

stringent need be the requirement for cancellation. On the other hand when the property of interest is the solvent HB acidity or basicity, the solvatochromic shifts of indicators that are able to accept or donate a hydrogen bond are compared to the shifts of a set of HB-inert indicators.

In a series of very careful studies Kamlet, Taft, and their collaborators determined π* for a large number of protic self-associating and nonassociating pure solvents including water, the lower alcohols, acetonitrile, and formamide (9, 10). Relevant results from their study are summarized in Table I along with a number of other related physical properties. It should be noted that the solutes used by Kamlet and ourselves (see Experimental Section) do contain functional groups that are hydrogen bond bases. For example solvatochromic measurements of the bulk solvent basicity of materials related to the solutes (benzene, β = 0.10; nitrobenzene, β = 0.30; anisole, β = 0.22; N,N-dimethylaniline β = 0.33) indicate that the ground states of these solutes are hydrogen bond acceptors.

In their preliminary evaluation of the π* values of HB acid solvents Kamlet et al. (9) essentially assumed that even though the solutes are HB bases, extensive cancellation in the effect of the solvent donor strength took place between the ground and the excited states and for other reasons the frequencies of maximum absorption did not shift significantly even when the solute accepted a hydrogen bond from a protic solvent. As an extreme example consider the indicator, 4-nitroanisole. Both the nitro and methoxy groups are hydrogen bond bases and therefore the ground state will be stabilized in an HB donor solvent. In the excited state the electron density on the nitro group increases, thereby enhancing its basicity; however, the electron density on the methoxy group in the excited state decreases, with a concomitant decrease in its basicity (11). The assumption was made that the net ground and excited state basicity is "conserved" and thus solvent HB acidity does not influence the ν_{max} of 4-nitroanisole. This

hypothesis was tested and found to be substantially correct (10).

To date there have been only a few studies of the π^* of solvent mixtures (12-14) and there are no studies of the π^* of mixtures containing water despite the importance of such systems for many theoretical and practical purposes of interest to analytical chemists including reversed-phase liquid chromatography (13). The data of Table I clearly point out that from the perspective of their hydrogen bond acid–base chemistry, the mixtures employed in liquid chromatography are very complex. The organic cosolvents range from non-HB acids (tetrahydrofuran) to methanol which is virtually as strong as HB acid as water. Similarly the liquids used in liquid chromatography may be only moderate acceptors, as is water, or rather strong bases, for example methanol. Even in the case of acetonitrile versus tetrahydrofuran, the recent factor analysis study of Chastrette et al. puts these two essentially aprotic liquids into two different classes of solvents (15). In order to make any progress in determining the solvent dipolarity/polarizability of such complex mixtures, it is essential to minimize the effect of these selective interactions on the measured property (14). In addition it must be recognized that even if the solute can be chosen so as to minimize the effect of hydrogen bonding to the solvent water, the alcohols and the other cosolvents will continue to interact with themselves by both type A and B hydrogen bond formation. The situation is further complicated by the possibility that to some extent strong self-association of the solvent can diminish the solvents availability for forming a hydrogen bond with a solute.

In contrast to the paucity of data on π^* for hydroorganic mixtures, there is a large body of solvatochromic data on a specific betaine indicator [4-(2,4,6-triphenylpyridinium)-2,6-diphenylphenoxide, denoted compound I], which is available through the very extensive work of Reichardt and his collaborators (16-18). Compound I is extremely sensitive to its environment as a consequence of the very large change in dipole moment upon excitation. Furthermore, due to the presence of the phenoxide group in the betaine, the ν_{max} of this indicator is also very strongly dependent on the HB acidity of the solvent. The solvent strength scale based on compound I is termed $E_T(30)$ and can be described by a combination of the Kamlet–Taft dipolarity parameter (π^*) and the related HB acidity scale (α) as follows (11):

$$E_T = 31.00 + 13.43\pi^* + 15.06\alpha \qquad (1)$$

$$n = 40, \ r = 0.984, \ \text{std dev} = 1.65$$

This equation holds for 40 solvents including aliphatic alcohols and other HB donors. The coefficients of π^* and α are essentially constant when an additional 26 aromatic and polyhalogenated solvents are added provided that the usual polarizability correction factor ($\delta = 0.5$ for polyhalogenated, $\delta = 1.0$ for aromatic solvents) is added to the regression equation.

Recently, Dorsey and his co-workers showed that for a very large number of solutes and several mobile-phase modifiers the logarithm of the capacity factor in reversed-phase liquid chromatography was well correlated with a normalized solvent shift parameter based on compound I (19, 20). The quality of analogous correlations using the Kamlet–Taft scale has not, as yet, been assessed due to the lack of such information for hydroorganic mixtures. However, for a fixed phase composition we have been able to relate reversed-phase retention to solute size, dipolarity, and hydrogen bond basicity (21, 22), and believe that Dorsey's correlation can be explained as a consequence of the strong covariance between the mobile phase HB acidity and cohesive energy density as measured by its solubility parameter. We have previously pointed out the existence of a correlation between the endothermic cavity

Table II. Comparison of π^* for Pure Solvents

Solute Properties

solute	1	2	4	32	45
$-s$	2.343	2.214	2.257	1.593	2.428
$\nu_0{}^a$	3.412	2.552	3.767	2.459	3.256
$\nu_0{}^b$	3.409	2.545	3.754		3.250

π^* Values

| | indicator | | | | | | |
solvent	1	2	4	32	45	av^c	std dev^d
water	1.11	0.80	1.21	1.39	1.19	1.17^e	0.18
methanol	0.60	0.62	0.60	0.73	0.61	0.61^f	0.01
acetonitrile	0.74	0.76	0.75	0.81	0.75	0.75^f	0.01
2-propanol	0.52		0.47		0.52	0.50	0.03
THF	0.61		0.65		0.53	0.60	0.06

^{a} Statistically determined ν_0 value by Kamlet and Taft (in μm^{-1}, ref 1). These values were employed to calculate the π^* values in this study. ^{b} The value of ν_0 measured in this work in cyclohexane. ^{c} The average of the π^* value obtained in this work. ^{d} The standard deviation of the measured π^* value. ^{e} The values for indicator 2 and 32 were excluded. ^{f} The value for indicator 32 was excluded.

parameter and the exothermic hydrogen bond acidity of such mobile phases (21).

Because the mobile phase is considered to be crucially important in reversed-phase liquid chromatography, that is, the lesser part of the overall free energy of transfer is derived from the stationary phase, we believe it appropriate to attempt to characterize hydroorganic mixtures of the more widely used organic cosolvents to better assess their overall dipolarity. To separate solvent hydrogen bonding effects from dipolar effects, one must choose indicators, in contrast to Reichardts' indicator, that have minimal sensitivity to solvent HB acidity.

EXPERIMENTAL SECTION

All solvents used in this work were HPLC grade and were used without further purification. The solvent mixtures were prepared by combining a known volume of each liquid. The results are thus reported as volume percent as taken; this is the usual composition scale in liquid chromatography. The density and other properties of the mixtures are well-known (23, 24). The solutes used in this work were either obtained commercially or were a gift from M. J. Kamlet. The indicators are p-nitroanisole [1], N,N-diethyl-m-nitroaniline [2], p-ethylnitrobenzene [4], N-methyl-o-nitroaniline [32], and o-nitroanisole [45]. The number in brackets refers to the Kamlet–Taft indicator designation (1). In either case the indicators were recrystallized and analyzed by reversed-phase HPLC before use. Dilute solutions (typically 0.5 mM or less) were prepared in the organic phase and then diluted with water. All spectroscopic measurements were carried out by the previously reported procedure (6). A GCA scanning spectrophotometer was used to make the measurements to ±0.2 nm. In order to check for solute self-association effects, each indicator was examined at concentrations that produced absorbances of approximately 0.5, 1.0, and 1.5 in the pure liquids. In all cases the standard deviation in the wavelength of maximum absorption was less than 0.3 nm. Consequently the solvent mixtures were examined with a single solute concentration chosen so that the absorbance was less than 1.5.

RESULTS AND DISCUSSION

The π^* values for the pure liquids measured in this work are summarized in Table II. π^* was computed as follows:

$$\pi^* = (\nu_{max} - \nu_0)/s \qquad (2)$$

where the values of ν_0 and s were taken from ref 1. Clearly the accuracy of the reported values will depend upon the accuracy of s and ν_0. The agreement between our values

Table III. Average π^* for Water–Cosolvent Mixtures

ϕ^a	methanol[b]	acetonitrile[d]	2-propanol[e]	tetra-hydro-furan[e]
0.0	1.17 (0.05)	1.17 (0.05)	1.17 (0.05)	1.17 (0.05)
0.1	1.16[c]	1.15[c]	1.17 (0.06)	1.16[c]
0.2	1.15 (0.06)	1.12 (0.04)	1.17 (0.05)	1.14 (0.03)
0.3	1.11 (0.04)	1.06 (0.05)	1.08 (0.04)	1.05 (0.01)
0.4	1.08 (0.03)	0.99 (0.04)	1.00 (0.04)	0.95 (0.01)
0.5	1.03 (0.03)	0.95 (0.04)	0.90 (0.06)	0.89 (0.00)
0.6	0.98 (0.03)	0.91 (0.04)	0.84 (0.06)	0.84 (0.01)
0.65	0.95[c]	0.87 (0.04)	0.81 (0.06)	0.81[c]
0.7	0.91 (0.02)	0.85 (0.03)	0.79 (0.06)	0.80 (0.02)
0.75	0.87[c]	0.85 (0.03)	0.76 (0.05)	0.78[c]
0.8	0.82 (0.01)	0.84 (0.03)	0.74 (0.06)	0.76 (0.02)
0.85	0.79[c]	0.82[c]	0.71[c]	0.73[c]
0.9	0.74 (0.01)	0.80 (0.02)	0.66 (0.06)	0.70 (0.03)
1.0	0.60 (0.01)	0.75 (0.01)	0.50 (0.03)	0.60 (0.06)
1.0[f]	0.61 (0.03)	0.75 (0.03)	0.50 (0.04)	0.60[g]

^{a} Volume fraction of organic cosolvent. ^{b} The average is based on indicators 1, 2, 4, and 45. The value of indicator 2 was excluded for organic volume fractions less than 0.3. ^{c} Interpolated by a cubic spline data fit. ^{d} The average is based on indictors 1, 2, 4, and 45. The value of indicator 2 was excluded for organic volume fractions less than 0.1. ^{e} The average is based on indicators 1, 4, and 45. ^{f} This denotes the values obtained by Kamlet and Taft (2). ^{g} The standard deviation for this solvent was not reported.

(Table II) and those of Kamlet (Table I) is seen to be quite good in all cases, even though in general we did not use the same set of test solutes as employed by Kamlet.

The initial work of Kamlet and Taft on the measurement of π^* values of hydrogen bond donor solvents was based on the following observations: the spectrum of 4-nitroanisole is insensitive to solvent HB acidity (ν_{max} in the monohydric alcohols all fall within the narrow range 3.279–3.294 μm^{-1}). N,N-Diethyl-3-nitroaniline, 4-methoxynitrostyrene, and 1-ethyl-4-nitrobenzene are considered to be non-HB indicator solutes in HBD solvents because plots of ν_{max} against ν_{max}(4-nitroanisole) in amphiprotic solvents are collinear with the same plots in non-HBD solvents (1).

The data for each indicator in each solvent are available upon request. The average π^* values are summarized in Table III. The results of mutual correlation between each solute and the average are given in Table IV. A plot of the π^* for solute 4 against the average π^* value as the solvent composition is varied is presented in Figure 1. The solid line in each plot is the line of perfect agreement (zero intercept, unity slope). Given that the reproducibility of measurement ranges from 0.01 to 0.03 for each solute, this agreement is acceptable.

Ideally the above type of plot should be constructed with a reference indicator that has absolutely no propensity to hydrogen bond with the solvent system. Unfortunately all of the indicators used in this work, as well as in the initial study of Kamlet, contain one or more potential sites of differential ground- and excited-state hydrogen bond basicity. Indeed, all of the indicators used to determine π^* contain such groups. To validate the findings of their initial approach Kamlet et al. circumvented this problem by choosing non-HBA substituents (CF_3 and SF_5). In addition these electron-withdrawing groups deactivate the HB basicity of the benzene ring. Finally they developed a spectroscopic approach (the ^{13}C NMR shift of the meta carbon relative to the para carbon) which was quite insensitive to solvent HB acidity (10). They found good agreement in strong HB donor solvents between values of π^* based on the UV shift of indicators 1–4 and the results based on the magnetic resonance shift. Unfortunately the probes used for ^{13}C NMR studies cannot be used to measure the π^* of water due to their low solubility. In in the present work we rely upon the Kamlet UV indicator

Table IV. Analysis of Plots of π^* vs π^*_{av}

solute	intercept[a]	slope[b]	r^c	std dev[d]	n^e
		Methanol–Water			
1	0.08	0.886	0.9988	0.009	10
2[f]	0.10	0.874	0.991	0.022	9
4	−0.07	1.085	0.9981	0.012	12
32	0.013	1.19	0.9982	0.014	10
45	−0.01	1.023	0.993	0.007	12
		Acetonitrile–Water			
1	0.063	0.905	0.998	0.007	12
2[f]	0.17	0.81	0.989	0.013	11
4	−0.10	1.10	0.992	0.018	12
32	−0.24	1.43	0.997	0.013	11
45	0.014	1.025	0.994	0.014	12
		2-Propanol–Water			
1	0.088	0.899	0.997	0.012	10
4	0.007	1.01	0.995	0.020	10
45	−0.11	1.10	0.99	0.012	10
		Tetrahydrofuran–Water			
1	0.11	0.857	0.999	0.008	13
4[f]	−0.22	1.22	0.998	0.013	12
45	0.077	0.959	0.997	0.017	12

^{a} Intercept in least-squares analysis of π^* vs$_{av}$. ^{b} Slope obtained as in a. ^{c} Correlation coefficient of least-squares fit. ^{d} Root mean square deviation of the fit. ^{e} Number of data points used in the fit. ^{f} This indicates that one or two data points were omitted based on a large deviation from linearity in the fit. Note the data deleted from the fit are shown in Figure 1.
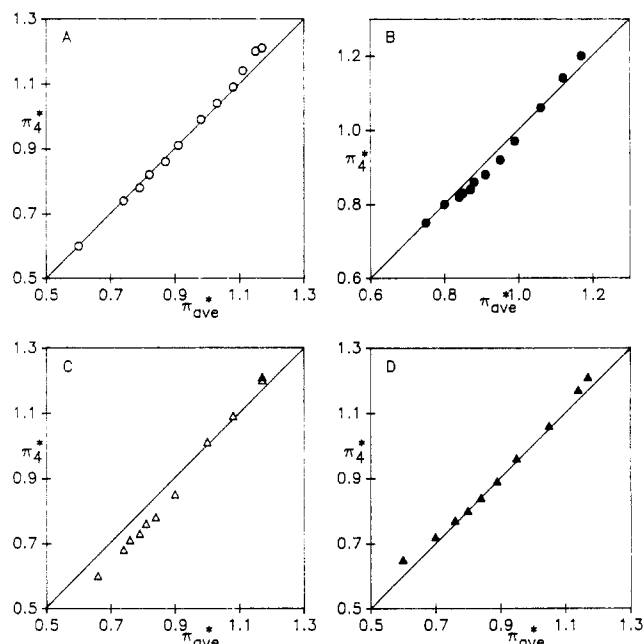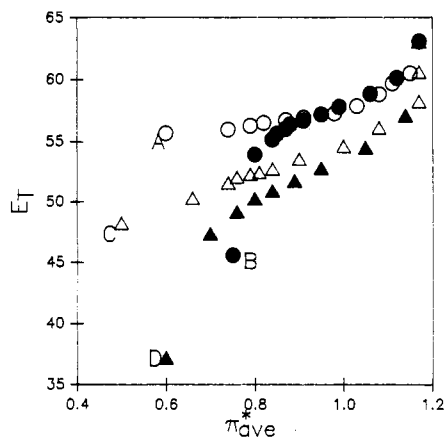

Figure 1. Plot of π^*_4 versus π^*_{av}: curve A, methanol–water mixtures; curve B, acetonitrile–water mixtures; curve C, 2-propanol–water mixtures; curve D, tetrahydrofuran–water mixtures. The solid line is the line of ideal fit.

method as an accurate measure of π^* in protic media. We did have some concern that the approach is not entirely reliable due to the fact that the experimental π^* of water, which is a strong HB acid, is underestimated by the best available correlations against dielectric constant and refractive index (π^*_{exp} = 1.09 in comparison to the predicted value of 0.95 by the equations in ref 6). However, indicator 4 (p-ethylnitrobenzene) gives very much the same π^* value as nitroanisole and nitroaniline (see Table II). Consequently, in view of the vast difference in the inductive effect of an ethyl group relative to the other substituents, we feel it is unlikely that there is much contribution of solvent HB acidity to the reported π^*
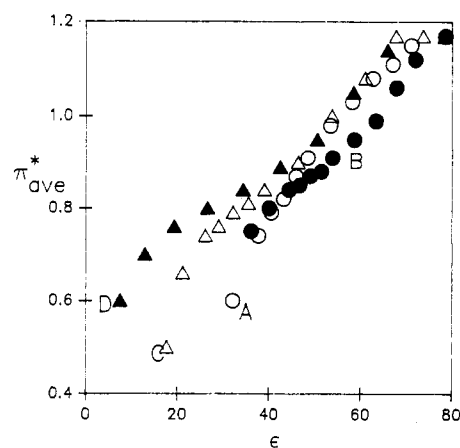
Figure 2. Plot of E_T against π^*_{av} for aqueous–organic mixtures: curve A, methanol–water mixtures; curve B, acetonitrile–water mixtures; curve C, 2-propanol–water mixtures; curve D, tetrahydrofuran–water mixtures. E_T data are from ref 17 and 18.

Figure 3. Plot of π^* against ϵ values for aqueous organic mixtures: curve A, methanol–water mixtures; curve B, acetonitrile–water mixtures; curve C, 2-propanol–water mixtures; curve D, tetrahydrofuran–water mixtures.

values. As will be discussed below, our mixture data support this view.

Plots similar to that shown in Figure 1 were examined for all solutes in all solvents. There is an excellent linear relationship for indicators 1, 4, 32, and 45 up to π^* equal to at least 1.0 in all of the solvent mixtures. Results of linear correlations are presented in Table IV. Indicator 2 behaved strangely when the volume fraction of methanol was less than 0.3. We believe that this is due to the very low solubility of this nonpolar solute in highly aqueous solutions. Note that indicator 2 behaved reasonably even in 0.1 volume fraction acetonitrile which for non-hydrogen-bond-accepting compounds is a stronger reversed-phase solvent than methanol. Consequently, we disregarded results with this indicator at the high water end of the plots. The indicators chosen here satisfy the criteria for implementing a solvatochromic comparison (*14*); that is, they correlate linearly, and thus the group of indicators can be described by a single solvent-dependent variable. Because the experimental data were transformed from an excitation energy coordinate to a π^* coordinate by means of eq 2, there are some systematic differences present (data not given) despite the fact that the average π^* for the pure organic solvents and for water are in good agreement with the literature (see Table I). For this reason, we decided to define an average using indicators 1, 4, and 45 and to restrict the study of 2-propanol and tetrahydrofuran to these indicators. Inspection of Table IV indicates that solute 32 gives a high slope versus the average π^*. In the case of solute 2, although we are convinced that it gives reliable information in organic-rich mixtures, we decided not to use it to characterize 2-propanol and tetrahydrofuran because it covaried so strongly in methanol and acetonitrile with the other indicators.

The strong covariance of solutes 1, 4, and 45 with one another argues against their sensitivity to solvent hydrogen bond acidity. If these solutes were able to sense differences in solvent HB acidity, then they would interact much more strongly with water than either acetonitrile or THF. Upon addition of water to the neat solvent, the cybotactic region about the solute would become enriched with water to a much greater extent than in an alcohol. Under these circumstances, one could not expect collinearity in plots of π^* of the different mixtures. This is in clear disagreement with the data of Tables III and IV.

In marked contrast to the plots shown in Figure 1, plots of E_T for the same mixtures versus the average π^* are rather complex (see Figure 2). This results from the simultaneous effect of a change in the solvent dipolarity/polarizability and hydrogen bond donor strength upon addition of water to the various media. In methanol and 2-propanol mixtures, plots

of E_T versus π^* are initially almost linear. In contrast, the first small amount of water added to acetonitrile or tetrahydrofuran causes a very sharp rise in E_T but only a modest increase in π^*; thus, these plots are quite convex. All four curves show a sharp concave bend between the last two data points as the solvent mixture approaches pure water. The final curvature is particularly evident in the case of tetrahydrofuran.

The data indicate that the order of *apparent* solvent *dipolarity* undergoes several changes when examined on the π^*-E_T coordinate system. For example, in the pure liquids the sequence of increasing dipolarity, based on the E_T values, is tetrahydrofuran < acetonitrile < 2-propanol < methanol. For the pure liquids, the sequence based on π^*, is 2-propanol < tetrahydrofuran < methanol < acetonitrile. The sequence by π^* is roughly in agreement with the dielectric constants of the pure substances (tetrahydrofuran < 2-propanol < methanol < acetonitrile). It has been demonstrated in a number of studies of the so-called select solvents (aprotic, nonaromatic, nonpolyhalogenated materials) that the primary determinant of π^* is the solvent dielectric constant with the refractivity being of subsidiary importance (*3-9*).

The relationship between the measured π^* and the dielectric constant of the mixtures is shown in Figure 3. The dielectric constants were obtained from several sources (*23, 25*). Where more than one data set was available, they were averaged by fitting all of the data to a third-order polynomial least squares regression. When data at a particular composition could not be located, we interpolated the existing data by a cubic splines method. Provided that the dielectric constant of the mixture is the only important factor, and assuming that the dielectric constant of the cybotactic environment is accurately represented by the bulk dielectric constant, all of the mixtures should fall on the same curve. This is definitely not the case. On the basis of the known relationship between π^* and refractive index, the variations in refractive index are too small to account for the displacement in the curves (*6*).

With the exception of the methanol data at high water content, the curves are displaced from one another in rough proportion to their bulk water content; that is, if we consider equidielectric mixtures (*23, 25*), the relative *bulk* water content would be tetrahydrofuran > 2-propanol > acetonitrile > methanol. There are two independent mechanisms that could act to cause displacement of the curves as seen in Figure 3. Water, being both very acidic and highly dipolar, will concentrate in the cybotactic region. It will be prone to do so more readily in a solvent such as THF, which is both less
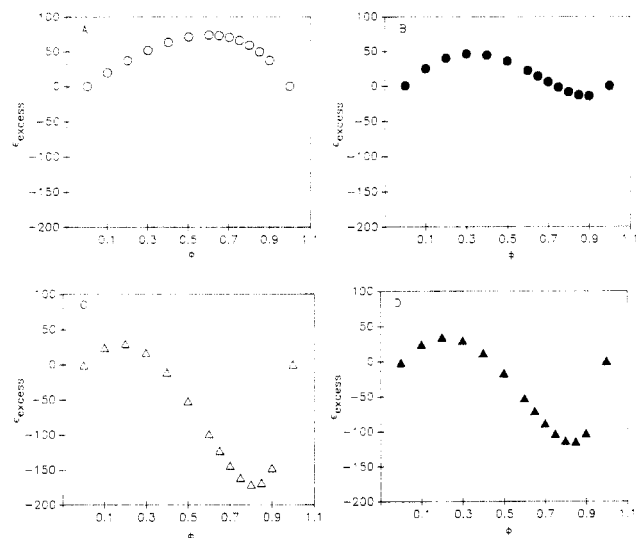
Figure 4. Plot of excess π^* against volume fraction of the organic cosolvent: curve A, methanol–water mixtures; curve B, acetonitrile–water mixtures; curve C, 2-propanol–water mixtures; curve D, tetrahydrofuran–water mixtures. All curves were computed from eq 4.

dipolar and less acidic, than is an alcohol. Whatever the mechanism, a high local water composition will generate a very dipolar microenvironment and cause an enhancement in the observed π^*. Kamlet and his co-workers have made the same point in their work on mixtures of aprotic nonpolar and aprotic dipolar solvents (12).

Analysis of plots of solvatochromic properties as a function of composition is quite complicated. Langhals (26, 27) has shown that for many systems, typically binary organic systems, plots of E_T against concentration can be linearized by use of the purely empirical expression

$$E_{T,mix} = E_{T,a} \log (C_b/C^* + 1) \qquad (3)$$

where C_b represents the molar concentration of solvent b and C^* is an adjustable linearizing parameter. Langhals found that his approach was not useful for hydroorganic mixtures. We also observed that π^* was not a linear function of the right-hand side of eq 3 for any value of C^*.

To examine the dependence of π^* on the composition of mixtures and relate π^* to dielectric constant and refractive index, Kolling made use of what he terms the "excess" π^* (28). There is also a large body of data on the dielectric properties of hydroorganic mixtures (29–33). It has been shown that excess functions are also useful for examining such data. These functions are defined as the difference between the observed property of the mixture and that predicted by an ideal model generally based on the behavior of a completely random mixture. This is arrived at by analogy to thermodynamic excess functions (34). Because our chief concern is to determine whether the π^* indicators were sensing the polarizability/dipolarity and not the HB acidity, we examined the excess π^* via use of the volume-fraction-weighted excess functions as suggested by the detailed theoretical analysis of Davis (32), rather than the mole-fraction-weighted approach taken by Kolling. In fact, there is little difference in these two approaches on the overall *shape* of the excess curves. Consequently, we define an excess solvatochromic property as follows:

$$\pi^*_{excess} = \pi^*_{mix} - \pi^*_{water}\phi_{water} - \pi^*_{org}\phi_{org} \qquad (4)$$

The excess E_T is computed in the same fashion. The data are given in Figures 4–6. The molar susceptibility (32) is defined as the product of the susceptibility, which is equal to $\epsilon - 1$, and the molar volume (V) of the mixture. According
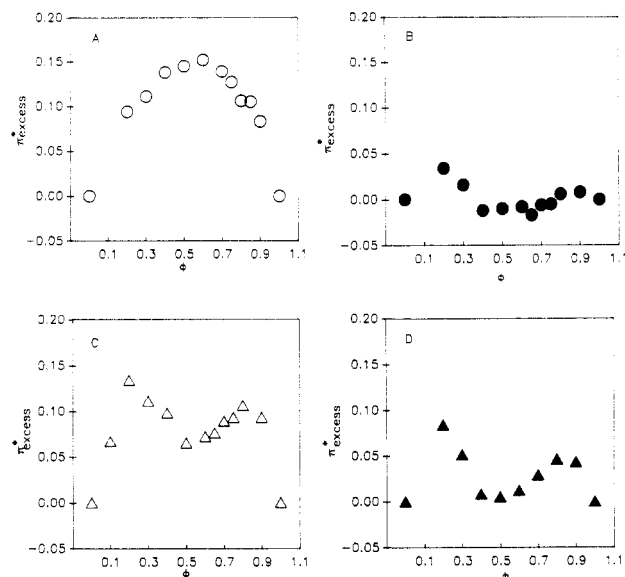
Figure 5. Plot of excess E_T against the volume fraction of the organic cosolvent: curve A, methanol–water mixtures; curve B, acetonitrile–water mixtures; curve C, 2-propanol–water mixtures; curve D, tetrahydrofuran–water mixtures. All curves were computed from eq 4.
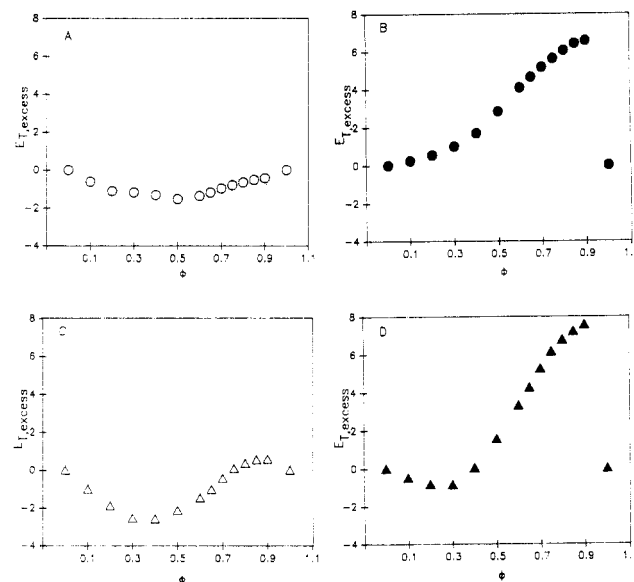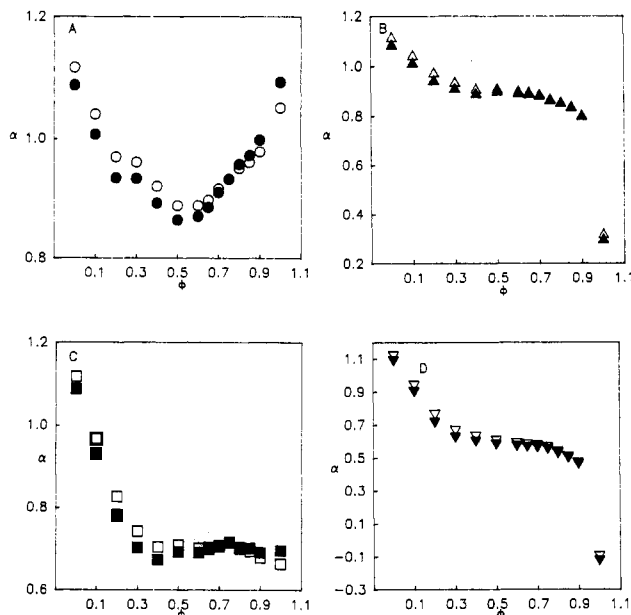

Figure 6. Plot of molar excess susceptibility against the volume fraction of the organic cosolvent: curve A, methanol–water mixtures; curve B, acetonitrile–water mixtures; curve C, 2-propanol–water mixtures; curve D, tetrahydrofuran–water mixtures. All curves were computed from eq 5.

to Davis (32) the most reasonable excess function to represent the dielectric property is

$$(\epsilon - 1)_{excess} = (\epsilon - 1)_{mix} - (\epsilon_{water} - 1)\phi_{water} - (\epsilon_{org} - 1)\phi_{org} \qquad (5)$$

The molar excess susceptibilities are given in Figure 6. It is evident that as the organic solvent is added in small amounts to water, both the molar susceptibility and π^* decrease more slowly than that predicted by random mixing. For methanol, 2-propanol, and tetrahydrofuran, E_T drops too rapidly, whereas there is almost no change seen in the data for acetonitrile. In all four hydroorganic systems, the gross shape of the curves of π^*_{excess} are in better accord with the excess susceptibility than is that of the excess E_T. In fact, for each of the π^* indicators the individual excess curves are quite similar to that of the average shown in Figure 4.

It is important to keep in mind that the dielectric constant is a bulk property of the mixture as a whole. The solvato-

Figure 7. Comparison of calculated α values from eq 7 and eq 8: curve A, methanol–water mixtures: curve B, acetonitrile–water mixtures; curve C, 2-propanol–water mixtures; curve D, tetrahydrofuran–water mixtures. The closed symbols denote values calculated from equation 7; the open symbols, from equation 8.

chromic properties, on the other hand, can only reflect the interaction of a solute with its immediate surroundings. Thus, the qualitative similarity in the shape of the excess π^* and molar susceptibilities is very significant. We interpret these results as indicating that the principal effect of changing the solvent composition on the observed value of π^* operates through the dielectric properties of the *local* medium about the solute. This adds to our confidence that the solute upon which we based the average π^* are not very sensitive to HB interactions. In contrast the excess properties of E_T depend quite strongly on both general electrostatic and solvent HB donor interactions.

One of the original motivations for this work was to investigate the solvent HB acidity parameter (α) of hydroorganic mixtures. Previous solvatochromic studies (*21*) of retention in reversed-phase liquid chromatography indicated the importance of the solute HB basicity (β) in establishing the solute capacity factor (k'). For example, we have shown that equations of the form

$$\log k'_2 = SP_0 + mV_2 + s\pi^*_2 + a\alpha_2 + b\beta_2 \qquad (6)$$

are most useful in explaining retention in reversed-phase chromatography. In this equation, V_2 is a measure of solute size (typically the molar volume or a hard core volume are used). The leading terms in the equation are invariably m and b. The coefficient b is related to the differential hydrogen bond acidity of the mobile and stationary phases (*21*).

Estimates of α can be obtained based on the assumption that eq 1 for pure solvents can be applied to a mixture. Thus we computed α_{mix} as follows:

$$\alpha_{mix} = (E_{T,mix} - 31.00 - 13.43\pi^*_{mix})/15.06 \qquad (7)$$

There are obviously a number of serious approximations and assumptions in using pure solvent regression results to interpolate data on mixed solvents. The resulting α values are shown in Figure 7 as the closed symbols. With the exception of the result in methanol mixtures, the qualitative trends are in good agreement with chemical intuition. Note the rapid rise in α for THF and CH_3CN mixtures upon addition of a small amount of water, a plateau region, and a final rise to the value of α in water. Although the trends, except for

methanol, are reasonable, there are considerable quantitative errors. The values of α calculated from eq 7 for water, methanol, 2-propanol, acetonitrile, and tetrahydrofuran are 1.16, 1.09, 0.74, 0.33, and −0.09, respectively. These should be compared to the experimental values of 1.17, 0.93, 0.76, 0.19, and 0.0 (see Table I). Recent work of Taft and co-workers indicates that α values generally have an uncertainty of ±0.10 unit (*34*). The peculiar behavior of the values for methanol–water mixtures—i.e., the unexpected minimum in the curve—might be related to the lack of fit of the correlation function for this solvent or to the existence of a complex species between water and methanol. To investigate this problem, we regressed E_T against the experimental π^* and α values for only these five solvents. The result is

$$E_T = 31.92(\pm3.8) + 11.42(\pm5.6)\pi^* + 15.95(\pm3.0)\alpha \qquad (8)$$

$$n = 5, r = 0.982, \text{ std dev} = 2.6$$

The value of α for methanol computed from this fit is 1.05, which is in good agreement with that computed from eq 7. We used eq 8 as the basis for the computation of α values for the mixtures. The results are shown in Figure 7 (open symbols). Clearly, both sets of curves are in good agreement.

It is altogether possible that methanol–water mixtures are weaker HB donors than either of the pure solvents. This could come about by the formation of a hydrogen bond complex between water and methanol as mentioned above. For example, Katz et al. have interpreted partitioning data in mixtures of water with methanol, acetonitrile, and tetrahydrofuran based on the formation of a 1:1 complex between water and the organic cosolvent (*36*). In view of the higher basicity of methanol relative to water, and its high acidity, it is possible that at an intermediate composition where such complexes are at their maximum concentration, the HB acidity could pass through a minimum.

Despite the above rationalization of the computed α values for methanol–water mixtures, we believe that there must be an error in the value of this mixture. This is based on our observation that in all correlations of solute retention in reverse-phase liquid chromatography on eight different types of columns, the magnitude of the b term invariably decreased as methanol was added to the mobile phase (*21*). The sign of b is such that an increase in solute basicity (β_2) leads to a decrease in retention. Thus, within the framework of the solvatochromic model of retention, the mobile phase acidity relative to the stationary phase must increase as water is added to the mobile phase. While this is consistent with the results for acetonitrile, tetrahydrofuran, and 2-propanol, it is clearly in disagreement with the α values computed for methanol–water mixtures. It should be noted that the direction of the changes in the measured values of π^* are entirely consistent with the variation of the s term (see eq 6) with solvent composition in reversed-phase chromatography. In view of the fact that the π^* scale is based on the average behavior of a set of indicators, whereas the computed α value is based on the performance of a single indicator, we believe that a specific solvation effect on Reichardt's betaine may be responsible for the apparent minimum in α. Extrema in plots of E_T versus solvent composition for other protic solvent mixtures are well-known (*37*).

LITERATURE CITED

(1) Kamlet, M. J.; Abboud, J. L.; Taft, R. W. *J. Am. Chem. Soc.* **1977**, *99*, 6027.
(2) Kamlet, M. J.; Abboud, J. L.; Abraham, M. H.; Taft, R. *J. Org. Chem.* **1983**, *48*, 2877.

(3) Abboud, J. L.; Taft, R. W. *Phys. Chem.* **1977**, *83*, 412.
(4) Brady, J. E.; Carr, P. W. *J. Am. Chem. Soc.* **1985**, *83*, 412.
(5) Brady, J. E.; Carr, P. W. *J. Phys. Chem.* **1982**, *86*, 3053.
(6) Brady, J. E.; Carr, P. W. *J. Am. Chem. Soc.* **1985**, *89*, 1813.
(7) Brady, J. E.; Carr, P. W. *Anal. Chem.* **1982**, *54*, 1751.
(8) Bekarek, K.; Jurina, J. *Collect. Czech. Chem. Commun.* **1982**, *47*, 1060.
(9) Abboud, J. L. M.; Kamlet, M. J.; Taft, R. W. *J. Am. Chem. Soc.* **1977**, *99*, 8325.
(10) Chawla, B.; Pollack, S. K.; Lebrilla, C. B.; Kamlet, M. J.; Taft, R. W. *J. Am. Chem. Soc.* **1981**, *103*, 6924.
(11) Kamlet, M. J., personal communication, June 1987.
(12) Kamlet, M. J.; Kayser, E. G.; Jones, M. E.; Abboud, J. L.; Eastes, J. W.; Taft, R. W. *J. Phys. Chem.* **1978**, *82*, 2477.
(13) Melander, W. R.; Horvath, C. In *High Performance Liquid Chromatography-Advances and Perspectives*; Academic: New York, 1980; Vol. 2, p 113.
(14) Kamlet, M. J.; Abboud, J. L.; Taft, R. W. *Prog. Phys. Org. Chem.* **1981**, *13*, 485.
(15) Chastrette, M.; Ragzmann, M.; Chanon, M.; Purcell, K. F. *J. Am. Chem. Soc.* **1986**, *107*, 1.
(16) Reichardt, C. In *Molecular Interactions*; Ratajczak, H., Orville-Thomas, W. J., Eds.; Wiley: Chichester, 1982; Vol. 3.
(17) Krygowski, T. M.; Wrona, P. K.; Zielkowska, U.; Reichardt, C. *Tetrahedron* **1985**, *41*, 4519.
(18) Krygowski, T. M.; Reichardt, C.; Wrona, P. K.; Wyszomirska, C.; Zielkowska, U. *Chem. Res. (S)* **1983**, 116.
(19) Johnson, B. P.; Khaledi, M. G.; Dorsey, J. G. *J. Chromatogr.* **1987**, *384*, 221.
(20) Johnson, B. P.; Khaledi, M. G.; Dorsey, J. G. *Anal. Chem.* **1986**, *58*, 2354.
(21) Sadek, P. C.; Carr, P. W.; Doherty, R. M.; Kamlet, M. J.; Taft, R. M.; Abraham, M. H. *Anal. Chem.* **1985**, *57*, 2971.
(22) Carr, P. W.; Doherty, R. M.; Kamlet, M. J.; Taft, R. M.; Melander, W.; Horvath, C. *Anal. Chem.* **1986**, *58*, 2674.
(23) Timmermans, J. *Physicochemical Constants of Binary Systems in Concentrated Solutions*; Interscience: New York, 1960; Vol. 4.
(24) Cheong, W. J.; Carr, P. W. *J. Liq. Chromatogr.* **1987**, *10*, 561.
(25) Moreau, C.; Dougheret, G. *Chem. Thermodyn.* **1976**, *8*, 403.
(26) Langhals, H. *Angew. Chem.*, *Int. Ed. Engl.* **1982**, *21*, 724.
(27) Langhals, H. *Nouv. J. Chim.* **1981**, *5*, 97.
(28) Kolling, O. W. *Anal. Chem.* **1985**, *57*, 1721.
(29) Kolling, O. W. *Anal. Chem.* **1984**, *56*, 2988.
(30) Balakrishnan, S.; Easteal, A. J. *Aust. J. Chem.* **1981**, *34*, 943.
(31) Nevecna, T.; Bekarek, V. *Collect. Czech. Chem. Commun.* **1986**, *51*, 1942.
(32) Davis, M. J.; Douhert, G. *Thermochim. Acta* **1986**, *104*, 203.
(33) Nevecna, T.; Vymetalova, J.; Bekarek, V. *Collect. Czech. Chem. Commun.* **1986**, *51*, 2071.
(34) Marsh, K. N. *Spec. Period. Rep. (Chem. Soc., London)* **1973**, *2*, Chapter 1.
(35) Taft, R. W., unpublished work, July 1987.
(36) Katz, E. D.; Ogan, K.; Scott, R. P. W. *J. Chromatogr.* **1986**, *352*, 67.
(37) Reichardt, C. *Solvent Effects in Organic Chemistry*, 1st ed.; Verlag Chemie: Weiheim, 1979.

CORRESPONDENCE

Alternating Current Plasma Detector for Selective Mercury Detection in Gas Chromatography

Sir: Gas chromatography (GC) coupled with element-specific detectors has been employed in many applications to simplify the interpretation of complex chromatograms. Desirable characteristics of an element-specific detector are that it should be highly specific for a wide range of elements, sensitive for these elements over a wide linear range, simple to construct and maintain, and stable under many application conditions. Spectroscopic-based detectors, such as plasma emission detectors (PED), satisfy these requirements and are commonly employed as element-specific detectors. There are three principal plasma emission sources employed for GC/PED, namely, microwave-induced plasma (MIP), inductively coupled plasma (ICP), and direct current plasma (DCP). The plasma emission detectors are well suited for element-specific detection due to their high selectivity, sensitivity, and compatibility with GC helium effluent flow rates (*1*). In addition, PED also have the advantage of being multielement detectors to provide valuable quantitative and qualitative data not readily available from the more conventional GC detectors. Selective detectors, such as the MIP detector, are commonly employed and exhibit high sensitivity and selectivity for both organometallics and nonmetals (*2–7*). However, these detectors do suffer from some disadvantages including solvent extinguishment and complexity in design.

This work describes the design, construction, and evaluation of a novel mercury-specific helium alternating current plasma detector (ACPD) for GC. The ACPD was designed to overcome some disadvantages suffered by other element-selective detectors. The power source employed for the detector produces a stable, self-seeding plasma. The detector design includes a tee configuration discharge tube and a heated fused silica-coated megabore capillary tube as the effluent transfer tube which reduces band broadening and offers improved sensitvity. The ACPD is evaluated for sensitivity, selectivity, and linear dynamic range with methylmercury(II) chloride and ethylmercury(II) chloride.

EXPERIMENTAL SECTION

Discharge Tube Design. A schematic diagram of the components of the ACPD is shown in Figure 1, while the plasma emission tube, which is an essential component of the ACPD, is shown in Figure 2. The body of the tube is in a tee configuration and constructed of $1/4$ in. o.d. × $1/8$ in. i.d. borosilicate glass tubing. The vertical electrode arms (3 in.) house the electrodes and transport the helium make-up gas to the plasma. The window arm (1.5 in. in length) is situated perpendicularly to the plasma discharge and electrode arm plane. The plasma discharge appears at the intersection of the arms; a quartz window or biconvex lens is fastened on the end of the window arm by silicon adhesive, forming an airtight tube.

An important feature of the tee design is the window arm in which the helium flow carries degradation products produced by the plasma discharge up and away from the window arm which results in the reduction of signal attenuation. Straight tube designs often were coated by degradation products, resulting in a loss in sensitivity due to blocked emission and has been a problem in previous work (*8*).

The airtight electrode holders, depicted in Figure 2, are a second feature of the discharge tube tee design. The holders are constructed of two $1/4$-in. Teflon tee unions (Cole-Parmer Instrument Co., Chicago, IL, catalog no. T-6374-42) attached to the end of each vertical electrode arm via Teflon $1/4$ in. ferrule nuts (Cole-Parmer Instrument Co., Chicago, IL, catalog no. J-6374-82). The perpendicular arm of each tee is fitted with a $1/4$ in. Teflon ferrule nut containing silicon rubber septa (Hamilton Co., Reno, NV, catalog no. 75805, 1 cm diameter) in which the electrodes are inserted. The electrodes are then positioned in the vertical